Resonance Raman evidence for the mechanism of the allosteric control of O2-binding in a cobalt-substituted monomeric insect hemoglobin

ARTICLE *in* BIOPHYSICAL JOURNAL · MARCH 1987

Impact Factor: 3.97 · DOI: 10.1016/S0006-3495(87)83335-0 · Source: PubMed

3 AUTHORS, INCLUDING:

Nai-Teng Yu
The Hong Kong University of Science and…

165 PUBLICATIONS **4,343** CITATIONS

SEE PROFILE

RESONANCE RAMAN EVIDENCE FOR THE MECHANISM OF THE ALLOSTERIC CONTROL OF O_2-BINDING IN A COBALT-SUBSTITUTED MONOMERIC INSECT HEMOGLOBIN

HELEN M. THOMPSON, NAI-TENG YU, AND KLAUS GERSONDE*
Georgia Institute of Technology, School of Chemistry, Atlanta, Georgia 30332;
**Rheinisch-Westfälische Technische Hochschule (RWTH), Abteilung Physiologische Chemie, D-5100 Aachen, Germany.*

ABSTRACT The substitution of iron for cobalt in the monomeric insect hemoglobin CTT (*Chironomus thummi thummi*) III does not alter the Bohr effect for O_2-binding. The cobalt substitution in this hemoglobin allows us to identify not only the O—O and Co—O_2 stretching mode but also the Co—O—O bending mode by resonance Raman spectroscopy. The assignments were made via $^{16}O_2/^{18}O_2$ isotope exchange. The modes associated with the Co—O—O moiety are pH-dependent. These pH-induced changes of the resonance Raman spectra are correlated with the $t \rightleftharpoons r$ conformational transition. At high pH (high-affinity state) two unperturbed O—O stretching modes are observed at 1,068 cm^{-1} (major component) and 1,093 cm^{-1} (minor component) for the $^{18}O_2$ complex. These frequencies correspond to split modes at 1,107 cm^{-1} and 1,136 cm^{-1} and an unperturbed mode at ~1,153 cm^{-1} for the $^{16}O_2$ complex. At low pH (low-affinity state) the minor component becomes the major component and vice versa. The Co—O_2 stretching frequency varies for ~520 cm^{-1} (pH 5.5) to 537 cm^{-1} (pH 9.5) indicating a stronger (hence shorter) Co—O_2 bond in the high-affinity state. On the other hand, the O—O bond is weakened upon the conversion of the low- to the high-affinity state. The Co—O—O bending mode changes from 390 cm^{-1} (pH 9.5) to 374 cm^{-1} (pH 5.5). In the deoxy form the resonance Raman spectra are essentially pH-insensitive except for a vinyl mode at 414 cm^{-1} (pH 5.5), which is shifted to 416 cm^{-1} (pH 5.5).

INTRODUCTION

Hemoglobins display a wide range of dioxygen affinities. Extremely high affinities have been observed for liver fluke hemoglobin (*Dicrocoelium dibranchiata* hemoglobin) (1, 2) and for leghemoglobin (3–5), which are both monomeric. The monomeric (6, 7) and the dimeric (6, 8, 9) Chironomus hemoglobins also exhibit considerably high dioxygen affinities, whereas low dioxygen affinities have been found for the tetrameric vertebrate hemoglobins (10). Some human mutant hemoglobins, like Hb M Iwate (11) and Hb Kansas (12), show extremely low dioxygen affinities. Ligand binding in many hemoglobins is controlled by allostery (namely cooperativity (13), polyphosphate effect (14), Bohr effect (15), and Root effect (16). Although numerous studies have been performed to elucidate the allosteric mechanism, the important information about the exact nature of the heme metal–ligand bonds in the different allosteric states of the hemoglobin is still lacking. As the human hemoglobin is a relatively complex allosteric system because of its quaternary structures and subunit heterogeneity, we employed a monomeric allosteric hemoglobin to identify and describe the relationship between tertiary structures and the heme metal–ligand bonds in more detail.

The hemoglobins from the larvae of the insect *Chironomus thummi thummi* are monomeric and dimeric. Of particular interest are the monomeric hemoglobins CTT III and CTT IV, which exhibit pH-dependent dioxygen affinities. The Bohr effect of CTT IV is larger than that of CTT III (7). A large body of structural (17, 18), thermodynamic (6, 7, 19, 20), and spectroscopic (21–35) data already exists for these monomeric insect hemoglobins. The influence of heme metal exchange and of porphyrin side group substitutions on the Bohr effect of these hemoglobins has also been investigated (25, 36). A single proton (Bohr proton) controls the binding of dioxygen (21). The changes in ligand affinity occuring over a range from pH 5 to 10 can be exactly described by the Bohr-effect curve (log P_{50}-vs. -pH plot) (7). Inflection points of the Bohr-effect curves at pH 7.1–7.4 indicate an alkaline Bohr effect. The Bohr proton forms a salt bridge between the COOH-terminal carboxyl group of Met H22 and the imidazole group of His G2, thus controlling the tertiary structure change (17, 21, 37). The replacement of the heme iron by cobalt decreases the dioxygen affinity ~250 times without

appreciable effect on the amplitude of the Bohr-effect curve (36). Therefore, the cobalt-substituted CTT III is a good model system for studying the allosteric mechanism. Electron spin resonance (ESR) studies on the cobalt-substituted form (36) and nuclear magnetic resonance (NMR) (28) and recent resonance Raman (35) investigations of the natural form of the monomeric insect hemoglobins have provided evidence that the pH-induced conformational changes, as indicated by the heme periphery, have nearly no effect on the electronic structure of the central metal in the deoxy state. However, in the oxy state larger changes of the electronic structure of the cobalt–dioxygen complex accompany the $t \rightleftharpoons r$ conformational transition (36). It was concluded on the basis of ESR results that both axial ligands, i.e., the proximal histidine and the dioxygen, interact reciprocally with the central cobalt atom, if the pH is changed. At low pH, because of the approach of the proximal histidine to the central cobalt atom, the σ-donor strength of the proximal imidazole increases, whereas that of the dioxygen simultaneously decreases. At high pH, due to the removal of the proximal histidine from the cobalt atom, both interactions show the opposite behavior, i.e., the proximal histidine–cobalt interaction decreases, whereas the dioxygen–cobalt interaction increases. Due to this interpretation the *trans*-effect of the axial ligands may be the main trigger effect in this simple allosteric protein.

As the hyperfine constants did not give any information about the nature of the O—O bond, we employed resonance Raman spectroscopy to measure the O—O stretching frequency, which is a direct indicator of the O—O bond strength (and thus O—O bond length) (38). Contrary to the oxy complex of the natural (iron) hemoglobins, the O—O stretching vibration in cobalt hemoglobins is enhanced and thus visible in the resonance Raman spectrum. In this paper, we detect for the first time the Co—O—O bending mode in a cobalt-substituted hemoglobin. Furthermore, the pH sensitivity of the ν(Co—O_2), ν(O—O) and δ(Co—O—O) vibrations are demonstrated. The resonance Raman spectra of the deoxy form of cobalt CTT III are pH-insensitive with the exception of a line in the range of 414–416 cm^{-1}, which is tentatively attributed to vinyl mode. These results point to the possibility that the heme electronic structures in the two conformation states of the unligated form are identical, in agreement with observations on the natural deoxy CTT III (35). On the other hand, the ligated form reflects the sensitivity of the central metal–ligand bonds to the conformation transition.

MATERIALS AND METHODS

Purification of Natural CTT III

Monomeric CTT III from the lymph of insect larvae of *Chironomus thummi thummi* was purified and identified as described elsewhere (7, 21, 30). The hemoglobin was desalted, lyophilized, and stored at −30°C in the met form.

Preparation of Cobalt Substituted CTT III

Preparation of cobaltous protoporphyrin-IX, isolation of globin, and reconstitution of CTT III with globin and cobaltous protoporphyrin-IX were carried out as described elsewhere (36). The solution of cobalt hemoglobin was desalted by gel filtration. The freeze-dried material was stored at −30°C.

Resonance Raman Spectroscopy

Experiments were performed on a sensitive multichannel vidicon detector Raman system which has been described elsewhere (39). A Krypton ion laser (model 171, Spectra-Physics Inc., Mountain View, CA) was used for excitation in the Soret-region at 406.7 or 413.1 nm. The samples are kept in a spinning quartz Raman cell to prevent local heating and to minimize photodissociation.

Preparation of Samples

Samples were prepared by dissolving 0.35 mg of the lyophilized cobalt hemoglobin in 300 μl 0.2 M buffers (citrate–phosphate buffer at pH 5.5 or Tris-HCl buffer at pH 9.5) to obtain a ~70 μM hemoglobin solution. Undissolved material was completely removed by centrifugation. The hemoglobin solution was carefully degassed by repeated evacuation and, after being flushed with oxygen-free nitrogen gas, was then transferred via a gas-tight syringe into a stoppered Raman-cell, which contained a minimum amount of sodium dithionite and was filled with prepurified nitrogen gas. The deoxy spectrum was measured under N_2 atmosphere. Dioxygen gas ($^{16}O_2$ or $^{18}O_2$, 99%, from Stohler Isotopes) was introduced into the Raman-cell after evacuation of the nitrogen gas to obtain the oxy spectra.

RESULTS

Resonance Raman Spectra of Deoxy Cobalt CTT III

Fig. 1 demonstrates the pH insensitivity of the resonance Raman spectra of deoxy cobalt CTT III. One exception is the line at 414 cm^{-1} (pH 5.5), which shifts to 416 cm^{-1} (pH 9.5). Since a vinyl bending vibration (at 414 cm^{-1}) has been identified via vinyl deuteration in cyano-met CTT III (40), we attribute this line in deoxy cobalt CTT III also to a vinyl bending mode.

Assignment of Resonance Raman Lines by Oxygen Isotope Exchange in Oxy Cobalt CTT III

Fig. 2 exhibits the oxygen isotope effect on the resonance Raman spectra of oxy cobalt CTT III at pH 9.5. In the lower frequency region (*top*), the cobalt–dioxygen stretching frequency, ν(Co—O_2), is identified at 537 cm^{-1} ($^{16}O_2$) by its shift to 519 cm^{-1} ($^{18}O_2$). In the lower panel two ^{18}O-^{18}O stretching frequencies appear at 1,068 and 1,093 cm^{-1}. We tentatively assign these Raman lines to two Co—O—O moieties, which differ in the geometry of the Co—O—O grouping. In the $^{16}O_2$ complex of cobalt CTT III the 1,068 cm^{-1} line is shifted to high frequency, i.e., a ^{16}O-^{16}O unperturbed stretching mode should be expected at ~1,122 cm^{-1} (41). However, as this mode undergoes vibrational resonance interactions with a porphyrin ring

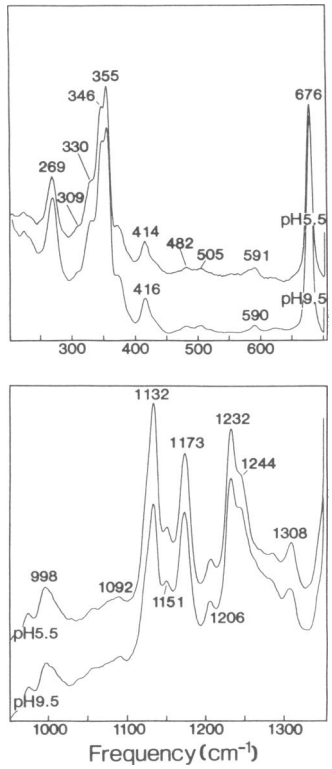

FIGURE 1 Resonance Raman spectra of deoxy cobalt CTT III at pH 5.5 and pH 9.5. Hb concentration, ~70 μM; buffers, 0.2 M Tris-HCl (pH 9.5) and 0.2 M citrate-phosphate (pH 5.5); λ_{exc} = 406.7 nm; laser power, ~20 mW; slit width, 100 μ; data integration time, 303 s, temperature, 22°C.

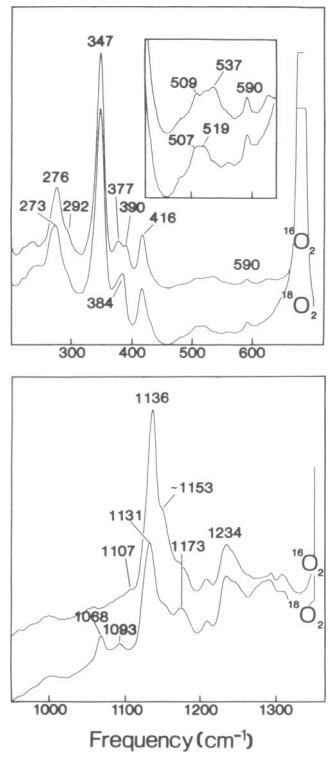

FIGURE 2 Resonance Raman spectra of oxy cobalt CTT III at pH 9.5 with oxygen isotope exchange $^{16}O_2$ for $^{18}O_2$. For experimental conditions see legend of Fig. 1. λ_{exc} = 413.1 nm for the low-frequency region and λ_{exc} = 406.7 nm for the high-frequency region; O_2 partial pressure, 2 atm for $^{16}O_2$ and 1 atm for $^{18}O_2$; temperature, 22°C.

mode, it is split into two lines at 1,107 and 1,136 cm^{-1}. Thus, it is this doublet in the $^{16}O_2$ spectrum that corresponds to the 1,068-cm^{-1} frequency in the $^{18}O_2$ spectrum. The other ^{16}O-^{16}O stretching frequency (unperturbed) is observed at ~1,153 cm^{-1}, which shifts to 1,093 cm^{-1} upon $^{18}O_2$ substitution. This interpretation is consistent with that already given for oxy cobalt sperm whale myoglobin and oxy cobalt hemoglobin A (41). The appearance of two O—O stretching lines with unequal intensities under all experimental conditions (in the low- and high-pH form, respectively) indicates that the two Co—O—O moieties, which are differently populated, exist in both conformation states of oxy cobalt CTT III, i.e., in the *t* and *r* conformations. The major component is characterized by the 1,068-cm^{-1} frequency ($^{18}O_2$) and the minor component by the 1,093-cm^{-1} frequency ($^{18}O_2$). Since there are two O—O stretching modes we also expect two Co—O_2 stretching frequencies. However, the quality of the low-frequency spectra does not allow the detection of the Co—O_2 stretching of the minor component.

Recently, some peculiar vibrational couplings between ν(O—O) and solvent/*trans* axial ligand modes in oxy Co porphyrins have been reported (42, 43). Such couplings can result in selective enhancement of specific internal modes of associates solvent or *trans* axial ligand, in addition to the ν(O—O) vibration. Therefore, caution must be exercised when one makes assignments of multiple oxygen isotope-sensitive lines to ν(O—O) modes. For oxy hemoproteins one must consider the possibility of selective enhancement (via vibrational couplings with ν[O—O] due to energy matching) of internal modes of proximal imidazole and/or H-bonded distal imidazole. In our studies of oxy Co CTT II (44) and oxy Co CTT III (this work) we find no evidence of such a peculiar enhancement. In fact, there exists strong evidence that supports our interpretation of two Co—O—O species for the two ν(O—O) modes at 1,136 and ~1,153 cm^{-1}. The strongest evidence comes from the resonance Raman spectrum of oxy Co CTT II at pH 5.5, where a single $\nu(^{16}O—^{16}O)$ line appears at 1,152 cm^{-1} and a single $\nu(^{18}O—^{18}O)$ line occurs at 1,080 cm^{-1}. Any vibrational resonance interactions between ν(O—O) and internal modes of proximal imidazole/H-bonded distal imidazole would result in more than one isotope-sensitive line in $^{16}O_2$ and/or $^{18}O_2$ spectra. Therefore, it is certain that the 1,152-cm^{-1} $\nu(^{16}O—^{16}O)$ line represents one Co—O—O species in the low affinity (pH 5.5) form of oxy Co CTT II. A nearly complete transition occurs in going from pH 5.5 to 9.5, causing the disappearance of the 1,152-cm^{-1} line and the appearance of a strong 1,134-cm^{-1} line, which represents a different Co—O—O species at high-affinity form (pH 9.5). In view of the work by

Kincaid et al. (43), the extremely weak feature at 1,105 cm^{-1} in the pH 9.5 spectrum of oxy Co CTT II (44) might be the internal vibration of imidazole or porphyrin. The spectral features in the spectrum of oxy Co CTT III (this work) are very similar to those in the spectrum of oxy Co CTT II except that the transition between the two Co—O—O species is not as complete as that found in oxy Co CTT II.

pH Dependence of Resonance Raman Spectra of Oxy Cobalt CTT III

In Fig. 3 the resonance Raman spectra of $^{16}O_2$ complexes of cobalt CTT III at pH 5.5 and 9.5 are compared. The high-pH form represents the high-affinity state, while the low-pH form represents the low-affinity state (36). In the low-frequency region of the pH 9.5 spectrum (see Fig. 3, (*top*)) the Co—O_2 stretching frequency occurs at 537 cm^{-1}. At pH 5.5 this vibrational mode is shifted to a lower frequency and is then hidden under a convolute of unassigned lines centered at ~520 cm^{-1}. The exact frequency of the pH-dependent line cannot be determined at low pH because of the low resolution of the overlapping modes and reduced signal-to-noise ratio in this frequency region. The frequency of the Raman line at 509 cm^{-1} (also not assigned) is not shifted by pH. It is, however, obvious that this line is intensity-enhanced at low pH. This intensity enhancement is probably caused by the pH-induced shift of the ν(Co—O_2) to lower frequency. Such an intensity enhancement has already been observed for an isotope-shifted vinyl mode coupling with the Fe—C—O bending mode in CTT III (45). In Fig. 3 (*bottom*) high-frequency region spectra (900–1,300 cm^{-1}) at high and low pH are compared. At pH 5.5 the intensity of the line at 1,153 cm^{-1} increases compared with pH 9.5, whereas the intensity at 1,136 cm^{-1} decreases. Thus, the population of the two above mentioned Co—O—O moieties changes with pH. As the two O—O stretching vibrations are present in the low-pH as well as in the high-pH form, it seems likely that the two Co—O—O moieties exist in both forms of oxy cobalt CTT III, whereas the population of the two Co—O—O moieties changes with pH. As no other Raman line in this region is pH-sensitive, the pH-induced change in intensity cannot originate from intensity enhancement of coupled modes. Therefore, we must assume that the pH-dependent change in intensity reflects the change in population of these moieties.

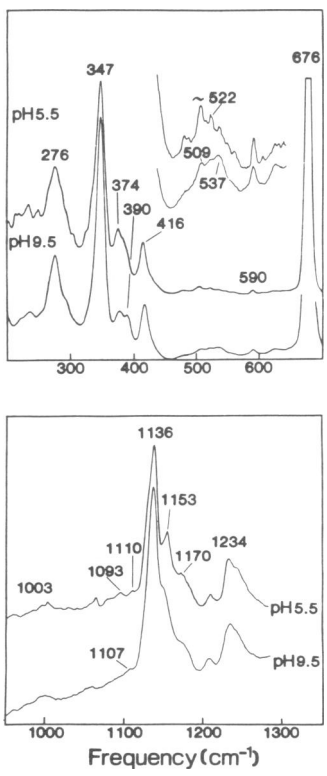

FIGURE 3 Comparison of resonance Raman spectra of oxy cobalt CTT III at pH 5.5 and pH 9.5. For experimental conditions see legend of Fig. 1. λ_{exc} = 413.1 nm for the low-frequency region and λ_{exc} = 406.7 nm for the high-frequency region; O_2 partial pressure, 2 atm for $^{16}O_2$.

Another pH-sensitive line occurs at 390 cm^{-1} (pH 9.5), which shifts to 374 cm^{-1} (pH 5.5). This pH-induced shift leads to an intensity enhancement of the 374-cm^{-1} line at low pH due to an overlapping with a pH-insensitive line of unknown origin. This 390 cm^{-1} at pH 9.5 is oxygen isotope-sensitive and shifts to 374 cm^{-1} with $^{18}O_2$ whereby the line is intensity enhanced by coupling. We assign this line at 390 cm^{-1} as a Co—O—O bending mode on the basis of the following arguments: (*a*) According to the finding on oxy phthalocyanato iron(II) (46) the Fe—O—O bending mode has been observed at 279 cm^{-1}, which is ~200 cm^{-1} lower than the Fe—O_2 stretching mode. In oxy cobalt CTT III the Co—O—O bending mode also occurs at lower frequency, i.e., it appears at a position that is ~150 cm^{-1} lower than the Co—O_2 stretching frequency. (*b*) The $^{16}O_2/^{18}O_2$ isotope shift in oxy phthalocyanato iron(II) is 8 cm^{-1}, whereas in oxy cobalt CTT III this shift is 6 cm^{-1}. With this assignment it is not surprising that this line is pH-dependent, as the Co—O_2 and the O—O stretching modes have also been found to be pH-dependent.

DISCUSSION

Oxygenated Forms of Cobalt Hemoglobins and Cobalt "Picket Fence" Porphyrin Model Complexes

One purpose of this investigation was the comparison of resonance Raman spectra of oxy cobalt CTT III with the previously reported spectra of oxy cobalt sperm whale myoglobin (41), oxy cobalt hemoglobin A (41), an oxy cobalt picket fence porphyrin (48). A comparison of oxy cobalt CTT III with oxy cobalt sperm whale myoglobin shows that most of the lines in the spectra, especially those that are due to porphyrin ring modes, are very similar. There exists one exception: a line at 439 cm^{-1}, which is

present in oxy cobalt sperm whale myoglobin, is completely missing in oxy cobalt CTT III. The vibrational modes associated with the cobalt–dioxygen moiety of the high-pH form of cobalt CTT III are strikingly similar to those of cobalt myoglobin. It is interesting to note that these vibrations are pH-insensitive in oxy cobalt myoglobin, which does not exhibit a Bohr effect at room temperature (47).

The vibrational modes of the cobalt–dioxygen moiety in the low-pH form of cobalt CTT III are similar to those found for the oxy cobalt picket fence porphyrin (48). These similarities in the ligand-associated vibrations between myoglobin and the high-pH form of CTT III and between picket fence porphyrin and the low-pH form of CTT III, respectively, indicate similar binding geometries for the bound dioxygen in each of these pairs.

pH-Induced Allostery in Oxy Cobalt CTT III

The pH 9.5 and 5.5 resonance Raman spectra of oxy cobalt CTT III show significant differences in three regions. The pH-dependent changes occur in the oxygen–oxygen stretching, the cobalt–oxygen stretching, and the Co—O—O bending modes. The spectral changes in the O—O stretching region reflect variations in the relative population of two different species of the bound dioxygen. The high-pH form (high-affinity state) exhibits a split mode at 1,107 and 1,136 cm^{-1} (the unperturbed stretching mode is expected at ~1,122 cm^{-1}). The low-pH form (low-affinity state) reveals a line at higher frequency (~1,153 cm^{-1}) for the ν(O—O). The transition from the low-affinity state (*t* conformation) to high-affinity state (*r* conformation) leads to an increase of the species with a longer (hence weaker) O—O bond and a decrease of the species with a shorter (hence stronger) O—O bond. As in CTT III distal histidine-O_2 interactions are absent, we believe that the O—O bond is most likely influenced by electronic affects. In the low-pH form (*t* conformation) the proximal histidine–cobalt interaction increases, resulting in a weakening of the σ-bond between dioxygen and cobalt, whereas π-bonding between dioxygen and cobalt increases.

The Co—O_2 stretching mode also exhibits a concomitant pH-dependence. In contrast to the O—O bond, the Co—O_2 bond is longer (hence weaker) in the low-affinity state, whereas it is shorter (hence stronger) in the high-affinity state. This reciprocal behavior of the Co—O_2 and the O—O bonds is the manifestation of the predominant effect of π-bonding.

Since the Co—O_2 and O—O bonds are influenced by the $t \rightleftharpoons r$ transition, we must expect that the Co—O—O bending is also affected by the conformational transition. The bending frequency is shifted from 390 cm^{-1} (pH 9.5) to 374 cm^{-1} (pH 5.5). The bending force constant depends on the nature of the Co—O_2 and O—O bonds and the nonbonding interaction between the terminal oxygen and the cobalt. ESR results on oxy cobalt CTT III led to the interpretation that in both conformations dioxygen is bound in the mode of ozonoid-type of bonding (36). However, in the high-affinity state of cobalt CTT III the Co—O—O bond angle is more inclined than in the low-affinity state, as already suggested from the hyperfine structure analysis of ESR spectra (36). Thus, the change from the more to a less inclined Co—O—O bond angle (change from stronger to weaker nonbonding interactions) results in a shift of the bending mode from 390 cm^{-1} (pH 9.5) to 374 cm^{-1} (pH 5.5). Since this is the first detection of the Co—O—O bending mode, further studies on oxy cobalt model compounds with known Co—O—O bond angle are necessary to correlate bending modes and Co—O—O bond angles.

For a detailed description of the pathway of conformational transmittance from the Bohr-proton site to the heme–ligand system one also needs to have information about the proximal histidine–cobalt bond. It is already known from ESR results that the proximal histidine is involved. The more direct evidence about the variations of the proximal histidine–cobalt bond strength await the detection of the histidine–cobalt stretching frequency by resonance Raman spectroscopy.

Effect of the Conformational Transition on a Vinyl Mode in Deoxy Cobalt CTT III

The only pH-sensitive vibration at 414–416 cm^{-1} in deoxy cobalt CTT III can be attributed to a vinyl group bending mode, $\delta(C_bC_\alpha C_\beta)$. Our tentative assignment is based on resonance Raman investigations of the natural CO- and cyanide-ligated CTTs III, which have been deuterated at the α- and the β-carbons of the vinyl groups (40, 45). However, the vinyl mode of the CO-ligated CTT III (observed at 417 cm^{-1}) exhibits in its vinyl-deuterated form a larger pH-induced shift (from 390 cm^{-1} at low pH to 379 cm^{-1} at high pH) (45) than the deoxy form of cobalt CTT III. It has been shown for the CO-ligated CTT III that the pH-dependent shift of the vinyl vibrational mode correlates with the alkaline Bohr effect, i.e., with the $t \rightleftharpoons r$ conformational transition. Thus, we must assume that the pH-induced $t \rightleftharpoons r$ transition also occurs in the deoxy state of cobalt CTT III. In this form, allosteric transition is reflected only by the heme vinyl–protein interactions, as the resonance Raman spectra are otherwise pH-insensitive. In the CO-ligated form of CTT III, this pH-induced shift of the vinyl resonance is five times larger, indicating more pronounced effects of the $t \rightleftharpoons r$ transition on the vinyl–protein interactions than in the deoxy form of CTT III. These findings in the resonance Raman spectra are completely consistent with earlier data that demonstrated that the deoxy form of CTT III shows a pH-induced $t \rightleftharpoons r$ conformational transition that is not transmitted to the central heme metal. Therefore, no changes of the ligand–heme metal interactions are observed for the deoxy CTT. For example, pH-induced changes of the hyperfine shifts

of the heme protons in deoxy CTT III have been observed by NMR, whereas the proximal histidine protons did not show pH-dependent hyperfine shifts (28). Earlier ESR studies demonstrated pH-independent cobalt and proximal imidazole nitrogen hyperfine structures, indicating that the cobalt–ligand system in deoxy CTT III is insensitive to the $t \rightleftharpoons r$ conformational transition (36). These results were recently confirmed by the finding of pH-independent O_2 on-rate constants for deoxy CTT III (49). In the oxy form, however, the $t \rightleftharpoons r$ transition is transmitted to the cobalt–ligand system as indicated by the characteristic changes in the O—O and Co—O stretching and Co—O—O bending modes.

We would like to thank Miss Sigrid Engels for excellent technical assistance.

This work was supported by grants from the National Institutes of Health (GM 18894 to N.-T. Yu), the medizinische Biophysik e.V. (to K. Gersonde), and the Fonds der Chemischen Industrie (to K. Gersonde).

Received for publication 18 February 1986 and in final form 18 August 1986.

REFERENCES

1. Sick, H., and K. Gersonde. 1985. Continuous gas depletion technique for measuring O_2-dissociation curves of high-affinity hemoglobins. *Anal. Biochem.* 146:277–280.
2. Smit, J. D. G., H. Sick, A. Peterhans, and K. Gersonde. 1986. Acid Bohr effect of a monomeric hemoglobin from *Dicrocoelium dendriticum*. Mechanism of the allosteric conformation transition. *Eur. J. Biochem.* 155:231–237.
3. Appleby, C. A. 1962. Oxygen equilibrium of leghemoglobin. *Biochim. Biophys. Acta.* 60:226–235.
4. Wittenberg, J. B., F. J. Bergerson, C. A. Appleby, and G. L. Turner. 1974. Facilitated oxygen diffusion. Role of leghemoglobin in nitrogen fixation by bacteroids isolated from soybean root nodules. *J. Biol. Chem.* 249:4057–4066.
5. Christahl, M., A. Raap, and K. Gersonde. 1981. pH dependence of oxy and deoxy cobalt-substituted leghemoglobin from soybean. An electron spin resonance study. *Biophys. Struct. Mech.* 7:171–186.
6. Sick, H., and K. Gersonde. 1969. Oxygen binding properties of some larval hemoglobins of *Chironomus* [Tendipes] *thummi*. *Eur. J. Biochem.* 7:273–297.
7. Gersonde, K., H. Sick, A. Wollmer, and G. Buse. 1972. Heterotropic allosterism of monomeric hemoglobins of *Chironomus thummi thummi*. *Eur. J. Biochem.* 25:181–189.
8. Overkamp, M. 1980. Untersuchungen zur allosterie in monomeren und dimeren hämoglobinen der zuckmucke *Chironomus thummi thummi* (Diptera, Insecta). Ph.D. dissertation. Rheinisch-Westfälische Technische Hochschule, Aachen, Germany. 65–84.
9. Zepke, H. -D., H. Sick, and K. Gersonde. 1981. Allostery of dimeric insect hemoglobin (CTT II). The influence of pH on the O_2 binding equilibria and kinetics. *Biophys. Struct. Mech.* 7(Suppl.):288.
10. Antonini, E., and M. Brunori. 1971. Hemoglobin and Myoglobin in their Reactions with Ligands. Elsevier North-Holland and Biomedical Press, Amsterdam. 235–254
11. Gersonde, K., M. Overkamp, H. Sick, E. Trittlevitz, and W. Junge. 1973. β-Chain allosterism in the frozen quaternary T-structure of hemoglobin M Iwate. *Eur. J. Biochem.* 39:403–412.
12. Atha, D. H., M. L. Johnson, and A. F. Riggs. 1979. The linkage between oxygenation and subunit association in human hemoglobin Kansas. Concentration dependence of the oxygen binding equilibriums. *J. Biol. Chem.* 254:12390–12398.
13. Monod, J., J. Wyman, and J. P. Changeaux. 1965. On the nature of allosteric transitions: a plausible model. *J. Mol. Biol.* 12:88–118.
14. Bartlett, G. R. 1980. Phosphate compounds in vertebrate red blood cells. *Amer. Zool.* 20:103–114.
15. Kilmartin, J. V. 1977. The Bohr effect of human hemoglobin. *Trends Biochem. Sci.* 2:247–249.
16. Perutz, M. F., and M. Brunori. 1982. Stereochemistry of cooperative effects in fish and amphibian hemoglobin. *Nature (Lond.)* 299:421–426.
17. Steigemann, W., and E. Weber. 1979. Structure of erythrocruorin in different ligand states refined at 1.4Å resolution. *J. Mol. Biol.* 127:309–388.
18. Weber, E., W. Steigemann, T. A. Jones, and R. Huber. 1978. The structure of oxy-erythrocruorin at 1.4Å resolution. *J. Mol. Biol.* 120:327–336.
19. Sick, H., and K. Gersonde. 1974. Ligand specific Bohr effect in hemoglobins. *Eur. J. Biochem.* 45:313–320.
20. Gersonde, K., L. Noll, H. T. Gaud, and S. J. Gill. 1976. A calorimetric study of the carbon monoxide Bohr effect of monomeric hemoglobins. *Eur. J. Biochem.* 62:577–582.
21. Sick, H., K. Gersonde, J. C. Thompson, W. Maurer, W. Haar, and H. Rüterjans. 1972. Bohr proton binding site in a monomeric hemoglobin: NMR study. *Eur. J. Biochem.* 29:217–223.
22. Trittlevitz, E., H. Sick, and K. Gersonde. 1972. Conformational isomers of nitrosylhemoglobin: ESR study. *Eur. J. Biochem.* 31:578–584.
23. Trittlevitz, E., H. Sick, K. Gersonde, and H. Rüterjans. 1973. Reduced Bohr effect in nitric oxide-ligated *Chironomus* Hemoglobin. *Eur. J. Biochem.* 35:122–125.
24. Twilfer, H., M. Overkamp, and K. Gersonde. 1976. Conformation-controlled *trans*-effect of the proximal histidine in hemoglobins. An electron spin resonance study of monomeric nitrosyl hemoglobins *Z. Naturforsch.* 31c:524–533.
25. LaMar, G. N., M. Overkamp, H. Sick, and K. Gersonde. 1978. Proton nuclear magnetic resonance hyperfine shifts as indicators of tertiary structural changes accompanying the Bohr effect in monomeric insect hemoglobins. *Biochemistry.* 17:352–361.
26. LaMar, G. N., D. B. Viscio, K. Gersonde, and H. Sick. 1978. Proton nuclear magnetic resonance study of the rotational position and oscillatory mobility of vinyl groups in allosteric monomeric insect hemoglobins. *Biochemistry.* 17:361–367.
27. LaMar, G. N., K. M. Smith, K. Gersonde, H. Sick, and M. Overkamp. 1980. Proton nuclear magnetic resonance characterization of heme disorder in monomeric insect hemoglobins. *J. Biol. Chem.* 255:66–70.
28. LaMar, G. N., R. R. Anderson, D. L. Budd, K. M. Smith, K. C. Langry, K. Gersonde, and H. Sick. 1981. Proton nuclear magnetic resonance investigation of the nature of solution conformational equilibriums of monomeric insect deoxyhemoglobins. *Biochemistry.* 20:4429–4436.
29. Christahl, M., and K. Gersonde. 1982. Structure-related changes of the electron spin resonance spectra of the monomeric nitrosyl hemoglobin IV from *Chironomus thummi thummi*. *Biophys. Struct. Mech.* 8:271–288.
30. LaMar, G. N., R. R. Anderson, V. P. Chacko, and K. Gersonde. 1983. High resolution proton NMR as indicator of a silent mutation in the heme cavity of a monomeric allosteric hemoglobin. *Eur. J. Biochem.* 136:161–166.
31. LaMar, G. N., R. Krishnamoorthi, K. M. Smith, K. Gersonde, and H. Sick. 1983. Proton nuclear magnetic resonance investigation of the conformation-dependent spin equilibrium in azide-ligated monomeric insect hemoglobins. *Biochemistry.* 22:6239–6246.
32. Yu, N. -T., B. Benko, E. A. Kerr, and K. Gersonde. 1984. The iron-carbon bond length in carbonmonoxy and cyanomet complexes of monomeric insect hemoglobins—a critical comparison between resonance Raman and x-ray crystallographic studies. *Proc. Natl. Acad. Sci.* USA. 81:5106–5110.

33. Kerr, E. A., N. -T. Yu, and K. Gersonde. 1984. Assignments of the Fe—N_ϵ(His) stretching mode in the resonance Raman spectra of a monomeric insect cyanomethemoglobin. *FEBS (Fed. Eur. Biochem. Soc.) Lett.* 178:31–31.
34. Prusakov, V. E., R. A. Stukan, R. M. Davidov, and K. Gersonde. 1985. Non-equilibrium state of a monomeric insect hemoglobin induced by γ-irradiation and detected by Mössbauer spectroscopy. *FEBS (Fed. Eur. Biochem. Soc.) Lett.* 186:158–162.
35. Kerr, E. A., N. -T. Yu, K. Gersonde, D. W. Parish, and K. M. Smith. 1985. Iron-histidine stretching vibration in the deoxy state of insect hemoglobins with different O_2 affinities and Bohr-effects. *J. Biol. Chem.* 260:12665–12669.
36. Gersonde, K., H. Twilfer, and M. Overkamp. 1982. Bohr-effect and pH dependence of electron spin resonance spectra of a cobalt-substituted monomeric insect hemoglobin. *Biophys. Struct. Mech.* 8:189–211.
37. Huber, R., O. Epp, W. Steigemann, and H. Formanek. 1971. Atomic structure of erythrocruorin in light of the chemical sequence and its comparison with myoglobin. *Eur. J. Biochem.* 19:42–50.
38. Yu, N. -T. 1986. Resonance Raman studies of ligand binding. *Methods Enzymol.* 130:350–409.
39. Yu, N. -T., and R. B. Srivastava. 1980. Resonance Raman spectroscopy of hemeproteins with intensified vidicon detectors: studies of low frequency modes and excitation profiles in cytochrome *c* and hemoglobin. *J. Raman Spectrosc.* 9:166–171.
40. Gersonde, K., N. -T. Yu, E. A. Kerr, K. M. Smith, and D. W. Parish. 1987. Heme-rotational disorder in monomeric allosteric cyanomet insect hemoglobins monitored by resonance Raman spectroscopy. *J. Mol. Biol.* (in press).
41. Tsubaki, M., and N. -T. Yu. 1981. Resonance Raman investigation of dioxygen bonding in oxycobaltmyoglobin and oxycobalthemoglobin. Structural implication of splittings of bound O—O stretching vibration. *Proc. Natl. Acad. Sci. USA.* 78:3581–3585.
42. Bajdor, K., K. Nakamoto, and J. R. Kincaid. 1984. Resonance Raman studies of dioxygen stretching vibrations in oxygen adducts of cobalt porphyrins. The importance of vibrational coupling. *J. Am. Chem. Soc.* 106:7741–7747.
43. Kincaid, J. R., L. M. Proniewicz, K. Bajdor, A. Bruha, and K. Nakamoto. 1985. Resonance Raman spectra of oxygen adducts of cobalt porphyrins. Enhancement of solvent and solute bands via resonance vibrational coupling. *J. Am. Chem. Soc.* 107:6775–6779.
44. Yu, N. -T., H. M. Thompson, D. Zepke, and K. Gersonde. 1986. Mechanism of the control of dioxygen binding in a dimreic cobalt-substituted insect hemoglobin. Resonance Raman evidence for cobalt-axial ligand bond changes. *Eur. J. Biochem.* 157:579–583.
45. Gersonde, K., E. A. Kerr, N. -T. Yu, D. W. Parish, and K. M. Smith. 1986. Resonance Raman investigation of CO-ligated monomeric insect hemoglobins. Direct evidence for reciprocal changes in iron-axial ligand bonds induced by allosteric transitions. *J. Biol. Chem.* 261:8678–8685.
46. Bajdor, K., H. Oshio, and K. Nakamoto. 1984. Observation of two oxygen-isotope sensitive bands in the low frequency resonance Raman spectrum of oxy(phthalocyanato)iron(II). *J. Am. Chem. Soc.* 106:7273–7274.
47. LaMar, G. N., D. L. Budd, H. Sick, and K. Gersonde. 1978. Acid Bohr effects in myoglobin characterized by proton NMR hyperfine shifts and oxygen binding studies. *Biochim. Biophys. Acta.* 537:270–283.
48. Mackin, H. C., M. Tsubaki, and N. -T. Yu. 1983. Resonance Raman studies of Co—O_2 and O—O stretching vibrations in oxy-cobalt hemes. *Biophys. J.* 41:349–357.
49. Gersonde, K., H. Sick, M. Overkamp, K. M. Smith, and D. W. Parish. 1986. Bohr effect in monomeric insect hemoglobins controlled by O_2 off-rate and modulated by heme-rotational disorder. *Eur. J. Biochem.* 157:393–404.